

# Proton aurora observed from the ground

Marina Galand\*, Supriya Chakrabarti

*Center for Space Physics, Boston University, MA, USA*

Available online 27 June 2006

---

## Abstract

Auroral keV proton precipitation is a significant-energy particle input upon the high-latitude ionosphere, often dominating in the polar cusp and the dusk sector of the equatorward auroral oval. A unique signature of proton precipitation is the Doppler-shifted H Balmer lines ( $H_{\alpha}$ ,  $H_{\beta}$ ) observable from the ground. These lines are emitted by energetic H atoms produced within the proton beam through charge-exchange processes. Their observations allow one to assess the location, dynamic evolution especially during magnetospheric substorms, and spectral characteristics of the source regions of the energetic protons projected to the high-latitude ionosphere. They also allow to identify the associated magnetospheric processes and to evaluate ionospheric perturbations induced by the energetic protons. The source regions include the cusp, the low-latitude boundary layer, the mantle, and the plasma sheet, including its dayside extension. If qualitative studies of proton aurora morphology and time variability are possible with photometric observations of hydrogen lines, quantitative assessment of H-emission brightness, and incident proton mean energy and flux, requires spectroscopic measurements of the H-emission profile. In this review paper, we report on the tremendous progress made in the past 20 years in the observational capability applied to proton aurora and in the modeling of energetic proton transport in the upper atmosphere, which is needed for quantitative analysis of the spectroscopic measurements of H emission. The current issues in the field are also discussed and suggestions for future directions are proposed. They include the deployment of chains of instruments dedicated to proton aurora studies along magnetic local time and geomagnetic latitude, such as high-spectral-resolution-imaging spectrographs and spectral imagers. Such campaigns would improve our understanding of the topology and dynamics of the magnetosphere, and provide, at dayside, the azimuthal extent of the reconnection region. Magnetically conjugate experiments and optical instruments dedicated to proton aurora observations in Antarctica are greatly encouraged. The contribution of atmospheric scattering to the H-spectral profiles needs to be further assessed and additional laboratory measurements of differential cross sections are required for a comprehensive understanding of the physics of proton aurora.

© 2006 Elsevier Ltd. All rights reserved.

*Keywords:* Proton aurora; H. Balmer; Auroral spectroscopy

---

## 1. Introduction

Auroral keV particle precipitation is an important energy source, which affects the electrodynamic properties, dynamics, thermal structures, as well as the composition in the high-latitude mesosphere and lower thermosphere region. Most of the auroral particle energy is carried into the high-latitude

---

\*Corresponding author. Space and Atmospheric Physics Group, Department of Physics, Imperial College, London, UK. Tel.: +44 20 75941771.

*E-mail addresses:* mgaland@bu.edu, m.galand@imperial.ac.uk (M. Galand), supc@bu.edu (S. Chakrabarti).

ionosphere by energetic electrons. Proton precipitation however occurs over all magnetic local times of the auroral oval and is often the dominant particle energy source in the cusp and at the equatorward boundary of the duskside auroral oval (e.g. Hardy et al., 1989; Creutzberg et al., 1988). The latter usually maps to the inner central plasma sheet. In the cusp and equatorward boundary of the duskside auroral oval, proton precipitation makes a significant contribution to, and, at times, even dominates the ionization (e.g. Basu et al., 1987; Galand et al., 2001; Lilensten and Galand, 1998; Galand et al., 2003) and the visible and far-ultraviolet aurorae (Ono et al., 1987; Rees, 1989; Frey et al., 2001, 2002; Lummerzheim et al., 2001; Galand et al., 2002; Ivchenko et al., 2004). Proton precipitation also induces ionospheric irregularities that give rise to SuperDARN E-region echoes. The locations of the equatorward boundaries of SuperDARN E-region backscatter and H emissions in the dusk–midnight sector of the auroral oval are coincident (Jayachandran et al., 2002). The cause of the precipitation of energetic protons varies with magnetospheric regions. On the nightside, the proton precipitation is diffuse, a result of scattering rather than acceleration. The origin of the scattering had been proposed to be field line curvature (Donovan et al., 2003), but further investigation needs to be conducted for a conclusive assertion.

Energetic electrons and protons do not interact in the same way within the atmosphere. The latter are very efficient ionizers with a key contribution of the induced electrons as source of excitation (e.g. Strickland et al., 1993; Galand and Richmond, 2001; Galand and Lummerzheim, 2004). It is thus crucial to separate the electron and proton components of auroral particle precipitation, in order to correctly assess ionospheric conductivities, heating, and composition changes, which is one of the important scientific issues of polar aeronomy, as stated by coupling, energetic, and dynamics of atmospheric regions (CEDAR)/phase III. In addition, as protons retain the large-scale structure more efficiently than electrons, imaging the proton aurora is an excellent probe for investigating magnetospheric substorms and magnetosphere–ionosphere coupling processes (e.g. Rees, 1989; Samson et al., 1992; Deehr and Lummerzheim, 2001; Immel et al., 2002; Mende et al., 2003; Zhang et al., 2004).

Hydrogen emissions resulting from excited H atoms produced within the incident proton beam are the spectroscopic signature of proton precipita-

tion. They are Doppler-broadened and -shifted, as the emitting H atoms, produced by charge-exchange reactions between energetic protons and atmospheric species, are energetic with a spread in energy. In the altitude region, where precipitating particles deposit their energy, the ambient H atom density is too low to produce any significant amount of auroral emissions from excitation by energetic particles, so the contribution from precipitating electrons or secondary electrons is negligible. Proton aurora is diffuse owing to the neutral component of the energetic beam whose path, independent of the magnetic field configuration, produces a spreading of the incident proton beam. In this paper, we use the terms “electron aurora” and “proton aurora” to distinguish the type of precipitating particles. Both types of aurorae have the full spectrum of auroral emissions produced by atmospheric atoms and molecules. The proton aurora has, in addition, the Doppler-shifted hydrogen emissions.

Vegard (1939, 1948) was the first to detect the presence of a Doppler-shifted component in spectral profiles of H Balmer emissions observed from the ground. This finding established the existence of proton precipitation in auroral region. It also provided the first evidence that aurorae were caused by particle precipitation. The presence of proton precipitation was later confirmed with higher spectral resolution of H emission measurements by Meinel (1951). Review papers on proton aurora include those by Eather (1967), McNeal and Birely (1973), Eather (1988), and Rees (1989). An overview of the history of measured and modeled hydrogen lines can also be found in the introduction section of Lanchester et al. (2003). In the 1960s and 1970s, H-emission spectral profiles were observed with about 1 nm spectral resolution. The change of the spectral shape of H emissions with viewing angles was established observationally and could be qualitatively explained using simple models. The profile varies from symmetric around the rest wavelength for viewing perpendicular to the magnetic zenith, to asymmetric with a Doppler-shifted peak for viewing along the magnetic zenith. The location of the proton aurora over the entire auroral oval was estimated using tilting-filter technique, and the temporal and spatial occurrence of the H emissions with magnetic activity was investigated (e.g. Vallance Jones et al., 1982; Creutzberg et al., 1988). The latitudinal spreading occurring in proton aurora was evaluated. McNeal and Birely (1973)

reviewed the laboratory measurements of cross sections associated with energetic  $H^+/H$  impacts. They found that, while major  $H^+/H$  impact cross sections on  $N_2$  and  $O_2$  were available, H Balmer emission cross sections or  $H^+/H$  impact cross sections on O were unreliable or still unavailable. If excitation of atmospheric species ( $N_2$ ,  $O_2$ , O) by proton precipitation was anticipated, the lack of many excitation cross sections was limiting quantitative analysis of the associated emissions. A crucial step for proton aurora modeling was achieved when Van Zyl and Neumann (1980) and Yousif et al. (1986) provided reliable H Balmer cross sections for  $H^+/H$  impact on  $N_2$  and  $O_2$ .

Fifteen years ago, Rees (1989) stated that one of the remaining problems in auroral physics is the relationship between proton and electron precipitation. If the characteristics of the optical spectrum resulting from proton precipitation into the atmosphere can be predicted with some confidence, it may become possible to separate the contributions of proton and electron excitation in auroral spectrum. Tremendous progress has been made since then in modeling and instrumental performance related to proton aurora. A special section in the Journal of Geophysical Research was dedicated to “proton precipitation into the atmosphere” emphasizing to the ionospheric and magnetospheric communities the role the energetic protons play in the upper atmosphere (Galand, 2001). In the present paper, we review the research conducted in the past two decades on proton aurora and focus on the ground-based observations and analysis of the  $H_\alpha$  (656.3 nm) and  $H_\beta$  (486.1 nm) Balmer emissions. After a short description of the experimental sites used, we first present photometric observations and summarize the findings. Subsequently, we discuss spectroscopic measurements and their analysis using comprehensive transport models. Finally, we provide recommendations for the future of this field.

## 2. Commonly used experimental sites

H emissions induced by precipitation of energetic protons originating from the plasma sheet have been observed from the dusk to the dawn sector of the auroral oval. Experimental sites over the past decades include Churchill, Fort Smith, Gillam, Thompson, Swan River, Pinawa, and Rankin Inlet located in Canada, Tromsø in Norway, Husafell in Iceland, Poker Flat in USA, Apatity in Russia, and Syowa in Antarctica. The location of these auroral

stations is given in Table 1, ordered by decreasing magnetic latitude. Typically, nighttime optical observation period extends from late August to beginning of May at Poker Flat Research Range (PFRR), and from early October to early April at Tromsø, but excludes near-full-moon periods.

Dayside measurements in darkness conditions of proton aurora have been carried out from the high-latitude stations of South Pole (US), Antarctica, and Adventdalen, Norway. Such measurements are made possible by the high geographic and geomagnetic latitude of these auroral stations (see Table 1). At Svalbard around winter solstice, the sun is well below the horizon ( $>8^\circ$ ) for more than two months; at winter solstice by local geomagnetic noon, the solar depression angle is  $13^\circ$  below the horizon. Observations from these stations include tracking the location and estimating the characteristics of the particle precipitation in the polar cusp, to which the solar wind has easy access through the magnetosheath and probing the low-latitude boundary layer (LLBL) and the dayside extension of the plasma sheet. The cusp is located at about  $\pm 75^\circ$  magnetic latitude during moderately disturbed conditions near local magnetic noon. It moves equatorward in response to both a southward turning of the IMF (or an intensification of the Bz component for southward IMF) and to a solar wind pressure increase. It is characterized by intense proton flux of low energies (e.g. Hardy et al., 1989; Henriksen et al., 1985, and references therein). Using all-sky instruments, different spatial regions of the auroral oval can be probed from these stations, from the dayside cusp to the midnight oval (Rees, 1989). At Svalbard, coordination with the nearby EISCAT Svalbard Radar (ESR) provides an assessment of the ionospheric state significantly perturbed by proton precipitation through E-region ionization (Vontrat-Reberac et al., 2001).

## 3. Photometric observations

### 3.1. Instruments and techniques

Photometers, equipped with interference filters to select auroral emissions such as H emissions, have been extensively used to characterize the latitudinal extent and dynamics of the proton and electron aurora. The most common instrument employed is the meridian scanning photometer (MSP) (e.g. Vallance Jones et al., 1982; Sato et al., 1986; Rees, 1989 and references therein; Samson et al., 1992;

Table 1  
Experimental sites where observations of proton aurora have been carried out from the ground over the past two decades

Station	Geographic latitude	Geographic longitude	Geomagnetic latitude	<i>L</i> value
Rankin Inlet, Canada	62.8°N	267.9°E	73.1°N	
Churchill, Canada	58.8°N	266.0°E	69.9°N	
Fort Smith, Canada	60.0°N	248.1°E	68.0°N	
Gillam, Canada	56.4°N	265.4°E	66.8°N	6.6
Thompson, Canada	55.7°N	262.1°E	66.4°N	
Tromsø, Norway	69.6°N	19.2°E	66.4°N	6.2
Husafell, Iceland	64.7°N	339.0°E	66.0°N	6.0
Poker Flat, Alaska	65.1°N	212.5°E	65.2°N	
Apatity, Russia	67.6°S	33.3°E	63.9°N	5.2
Swan River, Canada	52.1°S	258.8°E	62.4°N	
Pinawa, Canada	50.3°N	264.0°E	60.7°N	
Syowa, Antarctica	69.0°S	39.6°E	66.2°S	6.10
Adventdalen, Svalbard	78.2°N	15.8°E	74.9°N	~14
South Pole, Antarctica	90°S	—	74.3°S	13.1

The latitudinal chain of Canadian stations including Churchill, Thompson, and Swan River, was part of the Canadian International Magnetospheric Study (Vallance Jones et al., 1982). Fort Smith (northwest territories), Gillam (Manitoba), Pinawa (Manitoba), and Rankin Inlet (Nunavut) are nodes of the Canadian Auroral Network for the OPEN Program Unified Study (CANOPUS) network, as part of the NASA/International Solar-Terrestrial Physics Program (ISTP) (e.g. Samson et al., 1992; Donovan et al., 2003; Voronkov et al., 1999). Note that CANOPUS has been replaced by the NORthern Solar Terrestrial ARray (NORSTAR) project (<http://aurora.phys.ucalgary.ca/norstar>). The Tromsø station refers to the site of the European Incoherent SCATter Radar (EISCAT) at Ramfjordmøen, near Tromsø, Norway (Galand et al., 2003, 2004). Husafell, Iceland, was selected for a magnetically conjugated campaign (Sato et al., 1986). Poker Flat Research Range (PFRR) is a comprehensive auroral station with soon the addition of the US National Science Foundation (NSF)/Advanced Modular Incoherent Scatter Radar (AMISR) (Deehr and Lummerzheim, 2001; Lummerzheim and Galand, 2001). Apatity auroral station belongs to the Russian Polar Geophysical Institute (Borovkov and Chernouss, 2003). In the southern hemisphere, Syowa is the Japanese station in Antarctica (Sato et al., 1986; Ono et al., 1987; Takahashi and Fukunishi, 2001). Dayside proton aurora observations have been carried out from the very-high-latitude stations, including South Pole (US), Antarctica (Rees, 1989 and references therein), and Adventdalen on the Svalbard archipelago, Norway (e.g. Lorentzen and Moen, 2000; Lanchester et al., 2003).

Lorentzen and Moen, 2000; Deehr and Lummerzheim, 2001; Donovan et al., 2003).

One MSP has been operating at Poker Flat over the last two decades, and another at Svalbard over the last decade (see Table 1). They consist of a set of spatially scanning telescopes with optical interference filters that tilt on and off the auroral wavelengths of interest so as to allow the removal of the background—including the contamination by intense electron aurora—from the signal. The filters commonly used have a bandwidth around 0.5 nm. The  $H_{\beta}$  line is used for tracking the proton aurora. Even though the  $H_{\alpha}$  line is brighter than the  $H_{\beta}$  line, the close spectral proximity to the bright  $N_2$  1PG auroral emission and the OH(6,1) airglow emission makes it difficult to assess the hydrogen emission induced in proton aurora, especially on the night-side where hard ( $\geq 10$  keV) electron precipitation occurs. The other auroral wavelengths selected in the MSP are for identifying the hard component (OI 557.7 nm and  $N_2^+$  1NG 427.8 nm), and the soft ( $\leq 1$  keV) component (OI 630.0 and 844.6 nm, and

OII 732.0 nm) of electron aurora. It should be noted that proton precipitation also contributes to these channels (e.g. Deehr and Lummerzheim, 2001; Lummerzheim et al., 2001). The scan takes 16 s and is carried out along the north–south geomagnetic meridian covering the whole 180°-angle range. The data are usually presented as *keograms* (Eather et al., 1976) showing the magnetic meridian profile in a given channel (after removal of the background) as a function of time. An archive of the data covering the last decade at Svalbard and the last two decades at Poker Flat can be found at: <http://photon.gi.alaska.edu/home.html>. In the 1980s, in order to simplify the data acquisition, MSPs at the South Pole were replaced by slit cameras with films, each dedicated to one auroral emission (Rees, 1989 and references therein). Such a system directly provides a keogram over the whole campaign period. The first simultaneous two-point comparison of proton aurora brightness was proposed by Nicholson et al. (2003) between MSPs of two high-latitude stations, Poker Flat, Alaska, and

Gillam, Manitoba (see Table 1). This comparison demonstrates that the instruments produce qualitatively consistent measurements.

$H_{\beta}$ -monochromatic all-sky imaging systems equipped with filters for isolating selected auroral emissions have been deployed for proton aurora studies from Syowa station (Ono et al., 1987), with more recent versions including simultaneous background images (Takahashi and Fukunishi, 2001; Lummerzheim et al., 2003). Such instruments provide 2D-in-space spectral images, which are particularly useful for identifying the optimal temporal and spatial coincidence with flying-by satellites and deriving the combined space/ground-based dataset (Ono et al., 1987). Calibration is, however, still challenging, but these studies show that such an approach is possible. In the years to come, the technological issues are expected to be overcome. Such instruments would thus be superior to MSPs in allowing better temporal and spatial identification of auroral features in various spectral emissions.

### 3.2. Scientific achievements

Because of the diffuse nature of the H emissions and their relatively weak brightness compared to the electron aurora, the use of H emissions as an optical signature of proton precipitation has been slow to evolve. With the development of better interference filters and increased sensitivity detectors, MSPs operating at  $H_{\beta}$  have provided crucial information on the proton aurora over the past two decades. Through a combined satellite/ground-based dataset between in situ particle number and energy flux observations and (OI 557.7 nm and  $H_{\beta}$ ) MSP measurements, Ono et al. (1987) unambiguously showed for the first time the significant contribution of proton precipitation as an excitation source of the upper atmosphere at the equatorward boundary of the duskside auroral oval.

Research has also focused on the relative morphology and dynamics of proton and electron aurora, and the identification of the optical atmospheric signatures of magnetospheric regions and processes, especially during auroral breakup events and magnetospheric substorm periods (e.g. Vallance Jones et al., 1982; Sato et al., 1986; Samson et al., 1992; Voronkov et al., 2000; Wanliss et al., 2000; Deehr and Lummerzheim, 2001; Takahashi and Fukunishi, 2001). Two approaches have commonly been applied. The first one is based on the deploy-

ment of ground-based chain of MSPs, such as the latitudinal chain of  $H_{\beta}$  and OI 557.7 nm MSPs between Churchill, Thompson, and Swan River, Canada (see Table 1) (Vallance Jones et al., 1982; Creutzberg et al., 1988). The second approach appeals to a long timeline of MSP data from a given station (e.g. Deehr and Lummerzheim, 2001; Takahashi and Fukunishi, 2001 (along with a spectral imager); Donovan et al., 2003). Some studies combine both approaches, as described by Creutzberg et al. (1988) for deriving the mean distributions of proton and electron aurorae as a function of magnetic activity between 1800 and 0600 magnetic local time (MLT). All-sky camera and space-based particle observations are often used as complementary measurements to the MSP data. Here are few of the findings of these studies.

Using a combination of all-sky imager and MSP data from Poker Flat, Deehr and Lummerzheim (2001) found that during the growth phase of an auroral substorm, there are generally three precipitation regions separable in latitude: poleward arcs and bands associated with soft electron precipitation, electron arc at the trapping boundary associated with hard precipitation, and hydrogen, diffuse arc, extending over 100 km of latitude (see Fig. 1). The peak H emission moves equatorward more quickly than does the onset electron arc, and monotonically doubles in total intensity during equatorward motion, in a manner quite unrelated to the fluctuations in brightness of the onset arc. From the separation and very different temporal behavior of the onset arc and the peak proton precipitation, Deehr and Lummerzheim (2001) concluded that the auroral substorm originates poleward of the dipolar field lines and in the region of upward field-aligned current. This conclusion does not support the argument that the substorm onset begins from within the proton precipitation as suggested by theories of substorm onset that depend on resonance effects on closed, dipolar field lines (e.g. Samson et al., 1992 and references therein). The origin of the onset arc is still under debate today.

Donovan et al. (2003) developed a simple algorithm to estimate the ion-isotropy boundary from the latitudinal profiles of the  $H_{\beta}$  MSP channel. This boundary, identified as the b2i boundary in Defense Meteorological Satellite Program (DMSP) ion data (Newell et al., 1996), corresponds to the equatorward boundary of the proton aurora, an important magnetospheric transition that differentiates between

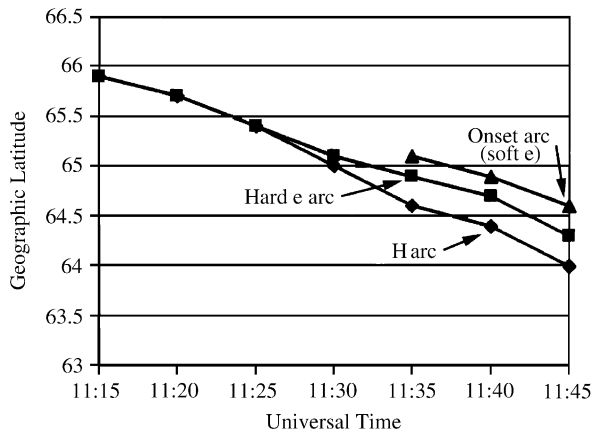


Fig. 1. Geographic latitude of the intensity maxima for three auroral arcs from PFRR meridian-scanning photometer record for February 1, 1990. The OI 557.7 nm and OI 630.0 nm were used for the electron-induced arcs (with lower values of the 630.0 nm/557.7 nm brightness ratio in the hard e-arc than in the onset arc). The 486.1 nm  $H_{\beta}$  emission was used for the H arc. The assumed altitude in all three cases was 110 km. Note that if a higher altitude were used for the less-energetic electron onset arc, the separation of the arcs would be even more apparent (Deehr and Lummerzheim, 2001).

regions of bounce trapping and strong pitch-angle scattering. The knowledge of its location provides a good indication of the amount of stretching on the magnetotail. Applying the algorithm to a 10-year MSP dataset from Gillam, Canada, Donovan et al. (2003) demonstrated a strong correlation between the magnetic latitude of the ion-isotropy boundary derived from MSP data and the inclination of the magnetic field as measured by GOES 8. Merging MSP  $H_{\beta}$  data sets from two high-latitude stations (Poker Flat and Gillam), Nicholson et al. (2003) demonstrated that the most equatorward extent of the proton aurora oval is offset duskward from the midnight meridian by approximately 45 min, and that the ion-isotropy boundary is symmetric within 2 h MLT of this point.

The pulsed proton events observed in the dayside aurora over Svalbard are attributed to the reconnection process, in which magnetosheath ions enter the magnetosphere on newly interconnected field lines. The field lines move in the direction of convection so that particles with different energies located on the same field line reach the ionosphere dispersed in both space and time. The pulsed nature of the auroral H emission is similar in temporal and spatial changes to the discrete dayside electron aurora associated with flux transfer events at the

magnetospheric boundary layer (Deehr et al., 1998; Lorentzen and Moen, 2000 and references therein).

MSP measurements have also been used as complementary dataset. While spectroscopic observations yield quantitative information on the incident protons through the analysis of the Doppler profile of H emissions, they are carried out over a few-degree field of view. As such, MSP measurements provide a crucial context on the latitude extent of the proton and electron aurora (e.g. Sigernes et al., 1996a; Deehr et al., 1998; Lorentzen and Moen, 2000; Lanchester et al., 2003). Photometric observations around auroral emissions including H emissions have also been used in support of rocket campaigns aimed at proton aurora studies to facilitate the launch decision and provide auroral context and conditions along the flight path (e.g. Søråas et al., 1974; Lorentzen et al., 1996).

It should be noted that a shortcoming of the photometric observations is the contamination by spectrally confined sources, such as galactic as well as geocoronal H emission, airglow, and auroral atmospheric emissions, such as OH and  $N_2$  1PG near  $H_{\alpha}$  (e.g. Galand et al., 2004). Background images obtained at a slightly different wavelength (outside the expected H-emission spectral extent in proton aurora) do not remove such a contamination. Spectral imaging and photometric imaging around specific atmospheric emissions allow the qualitative identification of such a contamination. For quantitative assessment of the H-emission brightness produced in proton aurora, spectroscopic observation is required.

## 4. Spectroscopic observations

### 4.1. Instruments and techniques

High-spectral-resolution ( $\leq 0.5$  nm) spectrographs have been used to acquire spectral profiles of  $H_{\alpha}$  and  $H_{\beta}$  emissions for quantitative analysis of the proton aurora from Svalbard (e.g. Henriksen et al., 1985; Lorentzen et al., 1998; Lanchester et al., 2003), Poker Flat (Henriksen et al., 1985; Lummerzheim and Galand, 2001), Tromsø (Galand et al., 2004), and Apatity (Borovkov and Chernouss, 2003). It should be noted that a key instrumental requirement for the observations of H-emission Doppler-shifted spectral profiles is the large value for the spectral range, greater than 10 nm for observations on the dusk- and nightside

of the equatorward oval where the hardest proton precipitation occurs.

Ebert–Fastie spectrographs (EFS) have been deployed at Poker Flat and Svalbard for H-emission observations in proton aurora (Fastie, 1952; Sivjee et al., 1979; Sigernes et al., 1996a, b; Lummerzheim and Galand, 2001). Such an instrument scans over the selected H Balmer spectral region. The 1-m  $H_{\beta}$  instrument used at Poker Flat had a full-width half-maximum (FWHM) of 0.43 nm and a field of view of  $7^{\circ}$  around the magnetic zenith (Lummerzheim and Galand, 2001). A profile was acquired every 16 s, but up to 15 scans are averaged together to improve the signal-to-noise ratio, yielding a time resolution of 4 min. Two EFS (0.5 and 1 m) measuring near  $H_{\alpha}$  or  $H_{\beta}$  have been used for observing proton aurora from Svalbard (Sigernes et al., 1996a; Deehr et al., 1998; Lorentzen et al., 1998). For a 1 mm slit, the FWHM of the H Balmer spectrograph is between 0.2 and 0.6 nm. The field of view is  $\sim 5^{\circ}$ . Each wavelength scan takes approximately 12 s, but the processed, useable profile is the sum of scans within a 2–4 min time segment.

Application of CCD detectors to spectroscopy allows simultaneous registration of all spectral elements of a line profile resulting in a large sensitivity gain. Such imaging spectrographs are currently the optimal instruments for high-spectral-resolution measurements of auroral hydrogen lines (Baumgardner et al., 1993; Borovkov and Chernouss, 2003). The high-throughput imaging Echelle spectrograph (HiTIES) has been used in proton aurora campaigns at Tromsø and Svalbard. It is an imaging spectrograph capable of simultaneously observing multiple wavelengths in a wide spectral region from 390.0 to 770.0 nm (Chakrabarti et al., 2001). HiTIES employs an Echelle grating, which is used at high orders and has a free spectral range of about 15 nm in a given order. Unlike conventional astronomical Echelle spectrographs, HiTIES uses a long input slit (45 mm) to increase its throughput. This instrument uses a “mosaic” of interference filters placed at the first image plane of the spectrograph to separate orders. One such instrument operated at Tromsø during two winter-long campaigns between 2001 and 2003 (Galand et al., 2003, 2004). The spectral resolutions in the  $H_{\alpha}$  and  $H_{\beta}$  windows of this instrument (FWHM) were 0.10 and 0.06 nm, respectively. The field of view of the processed profiles is  $2^{\circ}$  and the temporal resolution is 4 min. Another HiTIES spectrograph has also been operating at Svalbard since 2000 (Lanchester

et al., 2003; Ivchenko et al., 2004). The Balmer line selected is  $H_{\beta}$  with a FWHM of 0.13 nm. The field of view is  $8^{\circ}$ . The integration time can be as low as 10 s, but the temporal resolution of the processed proton aurora data is larger, of the order of the minute.

All the quantitative studies carried out with these instruments are based on observations obtained with a viewing centered on the local magnetic zenith. With such a configuration, the downward component of the precipitation is separated from the upward component through Doppler shift. In addition, this configuration minimizes any significant contribution to the hydrogen profile, of different incoming proton beams precipitating in the vicinity.

The wavelength calibration of the spectrograph in the  $H_{\alpha}$  and  $H_{\beta}$  windows is commonly performed using spectral lamps (hydrogen, neon, xenon, argon, krypton, and rubidium), and checked through the identification of airglow and auroral emission lines, and sunlight absorption lines. An example of photometric calibration is proposed by Galand et al. (2004). It was carried out using two different light sources: one whose absolute calibration is precisely known ( $C^{14}$  source) and the other, cross-calibrated to the first one, with a large spectral range and easily transportable to the experimental site (Tungsten lamp).

#### 4.2. Scientific achievements

Qualitative comparisons of simultaneous and magnetically co-located multi-instrument observations of proton aurora (electron density, H Balmer brightnesses and spectra, and in situ particle flux at the top of the atmosphere) have attested to the capability of high-resolution spectrographs to detect the presence of proton precipitation and confirmed the role of proton precipitation as a significant source of ionization in the high-latitude ionosphere (Galand et al., 2003).

The shape of the spectral profiles of H emissions observed from the ground along the magnetic zenith is blue shifted, as most of the emitting H atoms are propagating downward (as illustrated in Fig. 2). At low spectral ( $> 1$  nm) resolution, the Doppler shift of the peak is affected by the violet wing and the red-shifted wing is explained by the instrumental line broadening (Galand et al., 1998). At high spectral resolution ( $\leq 0.4$  nm), the red-shifted wing is distinguishable from the instrumental line broadening and

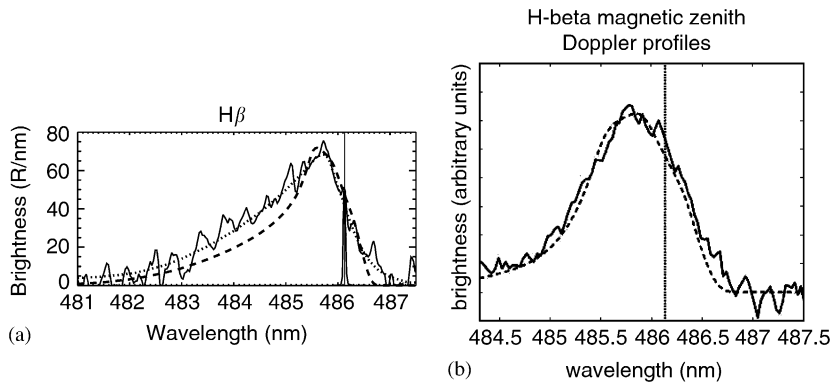


Fig. 2. (Left)  $H_{\beta}$  spectral profile in proton aurora observed at nightside from Tromsø (solid line). The dotted line represents the decontaminated Doppler-shifted profile. The dashed line shows the modeled profile obtained with a Maxwellian distribution in energy and a mean energy of 40 keV of incident protons. The H-lamp spectrum has been overplotted for reference (narrow line near  $H_{\beta}$  486.1 nm). The vertical thin solid line corresponds to the H Balmer line at rest (after Galand et al., 2004). (Right)  $H_{\beta}$  spectral profile in proton aurora observed at dayside from Svalbard (solid line). The dashed line is the modeled profile obtained from a  $H^{+}/H$  atom transport code using, as input, an ion flux measured simultaneously by DMSP over Svalbard. The vertical dotted line corresponds to the H Balmer line at rest (after Lanchester et al., 2003).

is evidence of back-scattered hydrogen atoms (Lummerzheim and Galand, 2001; Lanchester et al., 2003; Galand et al., 2004).

A spectral resolution of 0.1 nm is sufficient to identify and account for the contaminating OH-airglow emission, auroral  $N_2$  1PG emission, and geocoronal and galactic  $H_{\alpha}$  contribution in the  $H_{\alpha}$  spectral profiles observed in the duskside proton aurora (Galand et al., 2004). This finding opens up the possibility of using the strongest Balmer line for probing proton aurora. This is of particular interest on the dayside, as the  $H_{\alpha}$  profile is less affected by Rayleigh scattering of sunlight than the  $H_{\beta}$  profile for a given local solar depression angle. In addition, molecular band emissions are less significant at dayside than at nightside due to softer precipitation (e.g. Henriksen et al., 1985 and references therein).

On the nightside equatorward boundary of the auroral oval, the spectral profiles of H emissions observed from the ground are strongly asymmetric about the blue-shifted peak with a large violet wing. By comparison, the H-emission profiles measured at dayside are narrower with a violet wing of smaller spectral extent, as illustrated in Fig. 2 (Henriksen et al., 1985; Lanchester et al., 2003; Galand et al., 2004 and references therein). Deehr et al. (1998) observed a more pronounced variation in the wavelength of the peak of the Doppler-shifted line at dayside and a nearly symmetrical shape for the spectral profile. For further analysis of the Doppler-

shifted profiles observed in proton aurora, comprehensive  $H/H^{+}$  transport models are required.

## 5. Analysis of spectroscopic data using transport models

### 5.1. $H^{+}/H$ transport models

In the late 1980s, observational studies of proton aurora revealed the importance of energetic keV protons as a source of excitation of the upper atmosphere (e.g., Rees, 1989 and references therein). This finding raised the need for comprehensive models of proton transport for quantitative analysis of optical auroral data. The recent efforts invested in auroral proton studies have led to the development of comprehensive models describing the transport of an energetic incident proton beam in the upper atmosphere, its energy degradation and scattering, and its partial conversion to H atoms through charge-changing reactions. Several theoretical models of  $H^{+}/H$  transport have been developed recently, based on: 1D- or 3D-in-space Monte Carlo method (Kozelov, 1993; Lorentzen et al., 1998; Synnes et al., 1998; Gérard et al., 2000; Lorentzen, 2000; Solomon, 2001; Fang et al., 2004), or an explicit solution of the coupled  $H^{+}/H$  Boltzmann equations along the magnetic field line (Basu et al., 1993; Galand et al., 1998; Basu et al., 2001). Given the energy and pitch angle distribution of the incident proton intensity ( $=$  3D differential

number flux) at the top of the atmosphere (~600–800 km), the altitude profile of the number density of the atmospheric species, and the  $H^+/H$  impact cross sections on the atmospheric species, these steady-state models compute the proton and H-atom intensities over a range of altitudes, energies, and pitch angles. The brightness of auroral emissions induced by proton precipitation (e.g. Strickland et al., 1993; Lummerzheim et al., 2001; Galand and Lummerzheim, 2004) as well as the Doppler profiles of H emissions along the magnetic zenith (e.g. Lanchester et al., 2003) can be easily derived from these intensities.

To date, only two of these models (Lorentzen et al., 1998; Galand et al., 1998) have been used for the analysis of spectroscopic ground-based observations of the H Balmer lines in proton aurora. The first one is a 3D-in-space model including the spreading of the incident beam but neglecting collisional scattering, which modifies the shape of the H-emission profile. The second one is a 1D-in-space model which solves the transport along the magnetic field line and includes scattering of magnetic and collisional origins (Galand and Richmond, 1999; Lanchester et al., 2003).

## 5.2. Data analysis and findings

Analysis of high-spectral-resolution Doppler-shifted profiles of H emissions observed in proton aurora using comprehensive  $H^+/H$  transport models has yielded new findings in the past decade. Quantitative comparisons of simultaneous and magnetically co-located multi-instrument observations of proton aurora (electron density, H Balmer brightnesses and spectra, and in situ particle differential number flux flux at the top of the atmosphere) using transport models have attested to the capability of high-resolution spectrographs to identify the type of precipitating particles, and have been used to assess the H-emission Doppler-shifted profiles and to infer the ionospheric response to the particle precipitations (Galand et al., 2003; Lanchester et al., 2003). Such comparisons also show that the simulation contains the important physical processes that produce the H-line profiles, and confirms that measured changes in the shape of the hydrogen profiles are the result of changing energy input. The combination of high-resolution spectroscopic measurements and modeling provides a method of estimating the incoming energy and changes in energy flux of precipitating protons,

given the shape of the energy and pitch angle distributions (Lanchester et al., 2003).

The shape of the violet (blue shifted) wing, rather than the location of the peak of the blue-shifted  $H_\beta$  line profile (as illustrated in Fig. 2), is a suitable indicator of the mean energy of the precipitating proton beam—when one assumes a given shape of the energy and pitch angle distribution of the incident protons (Lummerzheim and Galand, 2001; Lanchester et al., 2003). While magnetic mirroring does not contribute to any significant red-shifted H emission (Galand et al., 1998), the red-shifted wing observed at high spectral resolution ( $\leq 0.4$  nm) is well reproduced by modeling through collisional angular redistribution (Lummerzheim and Galand, 2001; Lanchester et al., 2003; Galand et al., 2004).

The Balmer decrement, defined as the ratio of the total brightness of the  $H_\alpha$  to  $H_\beta$  lines in proton aurora, has been the focus of both experimental and theoretical studies for the last 40 years. This ratio could, in principle, yield information on the spectral characteristics of the incoming protons (Sigernes et al., 1996a). However, numerous uncertainties in measured and modeled  $H_\alpha$  and  $H_\beta$  line profiles still preclude us from using the Balmer decrement as an indicator of the precipitating proton mean energy (Galand et al., 2004).

Using the model developed by Lorentzen et al. (1998), Deehr et al. (1998) interpret the nearly symmetrical, narrow shape of the spectral profiles of H emissions observed on the dayside to be due to monoenergetic or narrow Gaussian energy spectra of the incoming protons. This is consistent with low-latitude satellite observations of ion fluxes (Sigernes et al., 1996a and references therein; Lorentzen et al., 1998). Dayside proton precipitation is indeed likely to be monoenergetic owing to the magnetospheric “velocity filter” resulting from dayside reconnection and convection (Lockwood and Smith, 1992; Onsager and Elphic, 1996 and references therein). 3D modeling of the  $H^+/H$  transport shows that the highest-energy ions could be separated spectroscopically from the lowest-energy population, assuming a precipitation region expanding over 75 km. Therefore, the velocity filter effect should be detectable from a latitudinal chain of spectrographs (Deehr et al., 1998). The H-emission spectrum observed at dayside is a direct measure of the instantaneous reconnection rate at the dayside magnetopause near the meridian of the observation (influenced by changes in the inter-

planetary magnetic field  $B_z$  component) through the detection of the temporal variation of the ion energy at a given location (Deehr et al., 1998; Lorentzen and Moen, 2000).

## 6. Summary and recommendations for future work

Since ground-based instruments make continuous observations at one location, they are well suited to study the variability and temporal evolution of the aurora. The Doppler-shifted H emissions are the spectroscopic signature of energetic proton precipitation. They are used for imaging the proton aurora, an excellent probe for tracking magnetospheric processes and regions, as well as for assessing the energy input to the ionosphere. While MSPs provide the morphology and dynamics of the proton aurora, the combination of high-resolution measurements with comprehensive modeling provides a method of quantitatively estimating the incoming energy and changes in energy flux of precipitating protons, assuming a given shape of the energy and pitch angle distributions of the incoming particles. To describe the interaction of protons with the upper atmosphere in a quantitative manner requires good spectral resolution ( $\leq 0.1$  nm for  $H_\alpha$  and  $\leq 0.4$  nm for  $H_\beta$ ) and appropriate temporal resolution ( $\leq 4$  min).

H emissions along with other auroral emissions have been used as optical signature of particle precipitation for probing the particle source and assessing magnetospheric processes occurring during various phases of geomagnetic substorms (see Section 3.2). If today there is some consensus on the main phase, the magnetospheric mechanism associated with the substorm onset is still under debate (Deehr and Lummerzheim, 2001), and further observations are needed to challenge the various, proposed theories. The relative extents of proton and electron aurora, and their dynamics have been mainly observed over a limited MLT sector at a time. Synoptic dataset over a larger MLT range—along with magnetic latitude coverage—would better constrain our ability to comprehend the magnetospheric configuration and evolution. For example, multi-point measurements of the ion-isotropy boundary—as illustrated by Nicholson et al. (2003) using two auroral stations separated in local time—will enhance our understanding of the topology and dynamics of the inner magnetosphere. In addition, proton aurora campaigns between two geomagnetically conjugate pair stations would sig-

nificantly improve our understanding of magnetic topology and particle acceleration mechanisms. To date, only one such campaign, carried out between Syowa, Antarctica, and Husafell, Iceland (see Table 1), near local magnetic midnight using  $H_\beta$  and OI 557.7 nm MSPs, has been reported (Sato et al., 1986). Qualitative correlation in the behavior of proton aurora between both stations was found during auroral breakup phase. However, the departure from predicted geomagnetic conjugate latitudes has limited the impact of the study.

To address these issues related to substorm studies and reach the objectives, we have two recommendations. The first one is to develop, validate, and deploy a 2D, multicolor, all-sky imaging system operating simultaneously at  $H_\beta$  emission line and its background, as tested at Syowa Station, Antarctica (Takahashi and Fuku-nishi, 2001), and at Poker Flat, Alaska (Lummerzheim et al., 2003). At this stage, further development is required to overcome the technological and the still-challenging calibration issues. The optimum systems are high-resolution spectral imagers (2D in space and 1D in wavelength). These could be systems such as the HiTIES instrument operating in a scan mode. The second recommendation is to deploy a chain of optical instruments (MSPs, spectrographs, and imagers) probing the electron and proton aurora over a large range of MLT with a large geomagnetic latitude coverage along the same magnetic meridian, while carrying out more magnetically conjugate campaigns at various MLT. The instrument set would include spectral imagers and high-resolution imaging spectrographs for deriving information on the hardness of the proton precipitation (as explained in Sections 4 and 5). One place which has been underutilized in the past 15 years, but from which many observational campaigns have been carried out in the 70s and 80s (Eather, 1988; Rees, 1989 and references therein), is Antarctica. It is a key place for conjugate campaigns and it is hoped that the upcoming International Polar Year 2007–2008 will offer the opportunity to carry out proton aurora campaigns from this continent.

Quantitative analysis of the Doppler-shifted H-emission profiles in proton aurora has improved considerably the past decade with the development of more sensitive and high-spectral-resolution spectrographs, and the development of comprehensive transport models of energetic protons and H atoms in the upper atmosphere (see Sections 4 and 5).

However, some aspects of the H-emission profiles remain unsolved. While the shape of the dayside  $H_\beta$  profiles in proton aurora is well understood (Lanchester et al., 2003), the violet (blue shifted) wing of the observed H Balmer profiles at nightside is underestimated by models (Galand et al., 2003, 2004). The brightness of the H Balmer lines observed in both dayside and nightside sectors is not well reproduced by models, even when the latter are driven by simultaneous, magnetically co-located particle measurements (Lorentzen et al., 1998; Galand et al., 2003). The brightness ratio observed between  $H_\alpha$  and  $H_\beta$  lines in proton aurora, the *Balmer decrement*, is not explained by models, and the uncertainties on both modeled and measured ratios vitiate the use of the Balmer decrement for characterizing the mean energy of the incoming protons (Galand et al., 2004). It is crucial to solve these issues, in order to improve our ability to assess proton characteristics (mean energy and energy flux), and to infer the ionospheric response to proton precipitation, from the analysis of H Balmer spectral profiles. When the H-line analysis in proton aurora is well established and validated from ground, it will be a powerful tool for the assessment of the particle energy input from a space-based platform.

There is a crucial need for laboratory measurements, in particular of differential cross section of  $H^+$  and H impact on  $N_2$  and  $O_2$  at large scattering angles, and on O over the whole scattering-angle range. Balmer emission cross sections induced by energetic protons and H-atom impacts are also needed for  $H_\beta$  above 3 keV on  $N_2$  and  $O_2$ , and for both  $H_\alpha$  and  $H_\beta$  on O over the whole energy range. It is also important to assess the effect of the spreading of the beam on the H spectral profiles. This can be achieved using 3D models (Lorentzen, 2000; Fang et al., 2004), after inclusion of collisional and magnetic angular redistribution, to determine the contribution of spreading in the shape of the H spectral profiles. One significant issue, which has been ignored to date in models, is the contribution of atmospheric scattering on the H spectral profiles yielding extinction due to scattering out of the field of view and contamination from scattering into the field of view. The accurate assessment of such contributions requires comprehensive radiative transfer calculations. Until such calculations are performed, we can only rely on observations, which tend to show that these contributions are expected to be small (Eather and Jacka, 1966). Additional

experiments that would further constrain the problem include the simultaneous observation of proton aurora in two or more directions at high spectral resolution and at a given location, and the deployment of 2D, even 3D, spectral imaging system.

Combined experiments between incoherent scatter radars, high-resolution spectrographs near H Balmer lines, and in situ particle measurements from satellites or rockets have to be pursued to challenge the transport models and improve our ability to retrieve the ionospheric state from spectroscopic analysis in proton aurora. Often particle detectors onboard polar orbiting satellites, such as DMSP and Fast Auroral SnapshoT (FAST), have a low energy cutoff of a few tens of keV. Studies of ion population in the central plasma sheet found that in high-energy range ( $>$  few 10s of keV), the ion spectrum has a non-thermal power law tail that can be modeled by kappa distribution (Christon et al., 1991 and references therein). The presence of a high-energy tail in the proton spectra was confirmed by low-altitude particle measurements aboard the Polar Operational Environmental Satellite (POES) (e.g. Codrescu et al., 1997) and the Upper Atmosphere Research Satellite (UARS) (Sharber et al., 1993). In addition, Decker et al. (1995) showed that in modeling the differential upgoing electron fluxes in a combined electron/proton aurora that were observed on Dynamics Explorer 2 (DE-2) satellite, excellent agreement between the observed and modeling upgoing electron fluxes is obtained when a kappa distribution is used to extrapolate the observed proton spectra to energies beyond the cutoff energy of the instrument aboard DE-2. It is therefore critical that the spectral range for particle measurements aboard future satellites and rockets extends from few 10s eV to several 100s of keV. The measurement of the high-energy tail in the incident proton spectra, especially at dusk and nightside, would be extremely valuable for a better assessment of the violet wing of the H Doppler profiles in proton aurora.

Dayside observations of proton aurora have been carried out from South Pole and Svalbard. The ion-energy distribution observed from such a station reflects the instantaneous reconnection rate near the meridian of the observation. Observations in several directions from one or more stations would determine the azimuthal extent on the magnetopause of the reconnection region and the direction of the convection in the ionosphere (Deehr et al.,

1998). In addition, modeling predicts that it should be possible to observe the velocity filter in the cusp region from a chain of high-spectral-resolution spectrographs located at different geomagnetic latitudes along the same geomagnetic meridian. Finally, the development of a capability of spectroscopic observations of the Balmer H emissions under sunlit conditions would offer a larger coverage in MLT over all seasons. With less Rayleigh scattering of sunlight than at  $H_{\beta}$  and relatively small auroral contamination due to soft electron precipitation,  $H_{\alpha}$  is the most appropriate H Balmer line for dayside proton aurora studies under twilight conditions. A higher-spectral-resolution (0.012 nm) version of the HiTIES spectrograph, high-resolution imaging spectrograph using Echelle grating (HiRISE) (Pallamraju et al., 2002), has observed sunlit cusp, auroral arcs, and mid-latitude aurora in OI 630.0 nm emission (Pallamraju et al., 2001, 2004; Pallamraju and Chakrabarti, 2005, 2006). Such a technique applied to H emissions should allow round-the-clock observations of proton aurora.

### Acknowledgments

We are very grateful to C. Deehr, B. Lanchester, and D. Lummerzheim for their valuable comments on the manuscript. We would also like to thank J. Baumgardner for enriching discussions. This work was supported by NSF Grant ATM-0003175 and NASA Grant NAG5-12773.

### References

- Basu, B., Jasperse, J.R., Robinson, R.M., Vondrak, R.R., Evans, D.S., 1987. Linear transport theory of auroral proton precipitation: a comparison with observations. *Journal of Geophysical Research* 92, 5920–5932.
- Basu, B., Jasperse, J.R., Strickland, D.J., Daniell Jr., R.E., 1993. Transport-theoretic model for the electron–proton–hydrogen atom aurora. *Journal of Geophysical Research* 98, 21,517–21,532.
- Basu, B., Decker, D.T., Jasperse, J.R., 2001. Proton transport model: a review. *Journal of Geophysical Research* 106, 93–105.
- Baumgardner, J., Flynn, B., Mendillo, M., 1993. Monochromatic imaging instrumentation for applications in aeronomy of the Earth and planets. *Optical Engineering* 32, 3028–3032.
- Borovkov, L.P., Chernouss, S.A., 2003. Application of the I-PentaMAX CCD camera for auroral spectrum observations. In: Kaila, K.U., Jussila, J.R.T., Holma, H. (Eds.), *Proceedings of 28th Annual Optical Meeting*, vol. 92. Sodankylä Geophysical Observatory Publications, pp. 77–79.
- Chakrabarti, S., Pallamraju, D., Baumgardner, J., Vaillancourt, J., 2001. HiTIES: a high throughput imaging Echelle spectrograph for ground-based visible airglow and auroral studies. *Journal of Geophysical Research* 106, 30,337–30,348.
- Christon, S.P., Williams, D.J., Mitchell, D.G., Huang, C.Y., Frank, L.A., 1991. Spectral characteristics of plasma sheet ion and electron populations during disturbed geomagnetic conditions. *Journal of Geophysical Research* 96, 1–22.
- Codrescu, M.V., Fuller-Rowell, T.J., Roble, R.G., Evans, D.S., 1997. Medium energy particle precipitation influences on the mesosphere and lower thermosphere. *Journal of Geophysical Research* 102, 19,977–19,987.
- Creutzberg, F., Gattinger, R.L., Harris, F.R., Wozniak, S., Vallance Jones, A., 1988. Auroral studies with a chain of meridian-scanning photometers 2. Mean distributions of proton and electron aurora as a function of magnetic activity. *Journal of Geophysical Research* 93, 14,591–14,601.
- Decker, D.T., Basu, B., Jasperse, J.R., Strickland, D.J., Sharber, J.R., Winningham, J.D., 1995. Upgoing electrons produced in an electron–proton–hydrogen atom aurora. *Journal of Geophysical Research* 100, 21409–21420.
- Deehr, C.S., Lummerzheim, D., 2001. Ground-based optical observations of hydrogen emission in the auroral substorm. *Journal of Geophysical Research* 106, 33–44.
- Deehr, C.S., Lorentzen, D.A., Sigernes, F., Smith, R.W., 1998. Dayside auroral hydrogen emission as an aeronomic signature of magnetospheric boundary layer processes. *Geophysics Research Letters* 25, 2111–2114.
- Donovan, E.F., Jackel, B.J., Voronkov, I., Sotiirelis, T., Creutzberg, F., Nicholson, N.A., 2003. Ground-based optical determination of the b2i boundary: a basis for an optical MT-index. *Journal of Geophysical Research* 108 (A3).
- Eather, R.H., 1967. Auroral proton precipitation and hydrogen emissions. *Physics Review* 5, 207–285.
- Eather, R.H., 1988. Results from Antarctic optical studies. *Review of Geophysics* 26, 579–590.
- Eather, R.H., Jacka, F., 1966. Auroral hydrogen emission. *Australian Journal of Physics* 19, 241–274.
- Eather, R.H., Mende, S.B., Judge, R.J.R., 1976. Plasma injection at synchronous orbit and spatial and temporal auroral morphology. *Journal of Geophysical Research* 81, 2805–2824.
- Fang, X., Liemohn, M.W., Kozyra, J.U., Solomon, S.C., 2004. Quantification of the spreading effect of auroral proton precipitation. *Journal of Geophysical Research* 109.
- Fastie, W.G., 1952. Image forming properties of the Ebert monochromator. *Journal of Optical Society of America* 42, 647.
- Frey, H.U., Mende, S.B., Carlson, C.W., Gerard, J.-C., Hubert, B., Spann, J., Gladstone, R., Immel, T.J., 2001. The electron and proton aurora as seen by IMAGE-FUV and FAST. *Geophysics Research Letters* 28, 1135–1138.
- Frey, H.U., Mende, S.B., Immel, T.J., Fuselier, S.A., Clafin, E.S., Gérard, J.-C., Hubert, B., 2002. Proton aurora in the cusp. *Journal of Geophysical Research* 107.
- Galand, M., 2001. Introduction to the special section: proton precipitation into the atmosphere. *Journal of Geophysical Research* 106, 1–6.
- Galand, M., Lummerzheim, D., 2004. Contribution of proton precipitation to space-based auroral FUV observations. *Journal of Geophysical Research* 109 (A3), A03307.

- Galand, M., Richmond, A.D., 1999. Magnetic mirroring in an incident proton beam. *Journal of Geophysical Research* 104, 4447–4455.
- Galand, M., Richmond, A.D., 2001. Ionospheric electrical conductances produced by auroral proton precipitation. *Journal of Geophysical Research* 106, 117–125.
- Galand, M., Lilensten, J., Kofman, W., Lummerzheim, D., 1998. Proton transport model in the ionosphere: 2. Influence of magnetic mirroring and collisions on the angular redistribution in a proton beam. *Annals of Geophysics* 16, 1308–1321.
- Galand, M., Fuller-Rowell, T.J., Codrescu, M.V., 2001. Response of the upper atmosphere to auroral protons. *Journal of Geophysical Research* 106, 127–139.
- Galand, M., Lummerzheim, D., Stephan, A.W., Bush, B.C., Chakrabarti, S., 2002. Electron and proton aurora observed spectroscopically in the far ultraviolet. *Journal of Geophysical Research* 107, 1.
- Galand, M., Baumgardner, J., Chakrabarti, S., Løvhaug, U.P., Isham, B., Jussila, J., Lummerzheim, D., Evans, D., Rich, F., 2003. Proton aurora over EISCAT: optical signature and associated ionospheric perturbations. In: Sigernes, F., Lorentzen, D.A. (Eds.), *Proceedings of 30th Annual European Meeting on Atmospheric Studies by Optical Methods*, August 13–17, 2003. University Courses on Svalbard Publication, Longyearbyen, Norway, pp. 2–8, ISBN:82-481-0006-5, <http://www.unis.no/research/30AMProceedings.pdf>
- Galand, M., Baumgardner, J., Pallamraju, D., Chakrabarti, S., Løvhaug, U.P., Lummerzheim, D., Lanchester, B.S., Rees, M.H., 2004. Spectral imaging of proton aurora and twilight at Tromsø, Norway. *Journal of Geophysical Research* 109, A07305.
- Gérard, J.-C., Hubert, B., Bisikalo, D.V., Shematovich, V.I., 2000. A model of the Lyman-alpha line profile in the proton aurora. *Journal of Geophysical Research* 105, 15,795–15,806.
- Hardy, D.A., Gussenhoven, M.S., Brautigam, D., 1989. A statistical model of auroral ion precipitation. *Journal of Geophysical Research* 94, 370–392.
- Henriksen, K., Fedorova, N.I., Totunova, G.F., Deehr, C.S., Romick, G.J., Sivjee, G.G., 1985. Hydrogen emissions in the polar cleft. *Journal of Atmospheric and Terrestrial Physics* 47, 1051–1056.
- Immel, T.J., Mende, S.B., Frey, H.U., Peticolas, L.M., Carlson, C.W., Gérard, J.-C., Hubert, B., Fuselier, S.A., Burch, J.L., 2002. Precipitation of auroral protons in detached arcs. *Geophysics Research Letters* 29.
- Ivchenko, N., Galand, M., Lanchester, B.S., Rees, M.H., Lummerzheim, D., Furniss, I., Fordham, J., 2004. Observation of  $O^+$  ( $^4P$ - $^4D^0$ ) lines in proton aurora over Svalbard. *Geophysics Research Letters* 31, L10807.
- Jayachandran, P.T., MacDougall, J.W., St-Maurice, J.-P., Moorcroft, D.R., Newell, P.T., Prikryl, P., 2002. Coincidence of the ion precipitation boundary with the HF E region backscatter boundary in the dusk–midnight sector of the auroral oval. *Geophysics Research Letters* 29, 1256.
- Kozelov, B.V., 1993. Influence of the dipolar magnetic field on transport of proton/H-atom fluxes in the atmosphere. *Annals of Geophysics* 11, 697.
- Lanchester, B.S., Galand, M., Robertson, S.C., Rees, M.H., Lummerzheim, D., Furniss, I., Peticolas, L.M., Frey, H.U., Baumgardner, J., Mendillo, M., 2003. High-resolution measurements and modeling of auroral hydrogen emission line profiles. *Annals of Geophysics* 21, 1629–1643.
- Lilensten, J., Galand, M., 1998. Proton/electron precipitation effects on the electron production and density above EISCAT and ESR. *Annals of Geophysics* 16, 1299–1307.
- Lockwood, M., Smith, M.F., 1992. The variation of reconnection rate at the dayside magnetopause and cusp ion precipitation. *Journal of Geophysical Research* 97, 14,841.
- Lorentzen, D.A., 2000. Latitudinal and longitudinal dispersion of energetic auroral protons. *Annals of Geophysics* 18, 81.
- Lorentzen, D.A., Moen, J., 2000. Auroral proton and electron signatures in the dayside aurora. *Journal of Geophysical Research* 105, 12,733–17,745.
- Lorentzen, D.A., Deehr, C.S., Minow, J.I., Smith, R.W., Stenbaek-Nielsen, H.C., Sigernes, F., Arnoldy, R.L., Lynch, K., 1996. SCIFER—dayside auroral signatures of magnetospheric energetic electrons. *Geophysics Research Letters* 23, 1885–1888.
- Lorentzen, D.A., Sigernes, F., Deehr, C.S., 1998. Modeling and observations of dayside auroral hydrogen emission Doppler profiles. *Journal of Geophysical Research* 103, 17,479–17,488.
- Lummerzheim, D., Galand, M., 2001. The profile of the hydrogen  $H_\beta$  emission line in proton aurora. *Journal of Geophysical Research* 106, 23–31.
- Lummerzheim, D., Galand, M., Semeter, J., Mendillo, M.J., Rees, M.H., Rich, F.J., 2001. Emission of OI(630 nm) in proton aurora. *Journal of Geophysical Research* 106, 141–148.
- Lummerzheim, D., Galand, M., Kubota, M., 2003. Optical emissions from proton aurora. In: Kaila, K.U., Jussila, J.R.T., Holma, H. (Eds.), *Proceedings of 28th Annual Optical Meeting*, vol. 92. Sodankylä Geophysical Observatory Publications, pp. 1–5.
- McNeal, R.J., Birely, J.H., 1973. Laboratory studies of collisions of energetic  $H^+$  and hydrogen with atmospheric constituents. *Review of Geophysics* 11, 633–693.
- Meinel, A.B., 1951. Doppler-shifted auroral hydrogen emission. *Astrophysics Journal* 113, 50–54.
- Mende, S.B., Frey, H.U., Morosny, B.J., Immel, T.J., 2003. Statistical behavior of proton and electron auroras during substorms. *Journal of Geophysical Research* 108.
- Newell, P.T., Feldstein, Y.I., Galperin, Y.I., Meng, C.-I., 1996. Morphology of nightside precipitation. *Journal of Geophysical Research* 101, 10737–10748.
- Nicholson, N.A., Donovan, E.F., Jackel, B.J., Cogger, L.L., Lummerzheim, D., 2003. Multipoint measurements of the ion isotropy boundary. In: Kaila, K.U., Jussila, J.R.T., Holma, H. (Eds.), *Proceedings of 28th Annual Optical Meeting*, vol. 92. Sodankylä Geophysical Observatory Publications, pp. 37–40.
- Ono, T., Hirasawa, T., Meng, C.I., 1987. Proton auroras observed at the equatorward edge of the duskside auroral oval. *Geophysics Research Letters* 14, 660–663.
- Onsager, T.G., Elphic, R.C., 1996. Is magnetic reconnection intrinsically transient or steady-state? The Earth's magnetopause as a laboratory. *Eos Transactions of AGU* 77, 26,241.
- Pallamraju, D., Chakrabarti, S., 2005. First ground-based measurements of OI 6300 Å daytime aurora over Boston in response to the 30 October 2003 geomagnetic storm. *Geophysics Research Letters* 32, L03S10.
- Pallamraju, D., Chakrabarti, S., 2006. A brief overview of applications of Echelle spectrographs for ground-based passive remote sensing of daytime upper atmosphere

- emissions, *Journal of Atmospheric Solar–Terrestrial Physics*, this issue.
- Pallamraju, D., Baumgardner, J., Chakrabarti, S., Pedersen, T.R., 2001. Simultaneous ground-based observations of an auroral arc in daytime/twilighttime OI 630.0 nm emission and by incoherent scatter radar. *Journal of Geophysical Research* 106, 5543–5549.
- Pallamraju, D., Baumgardner, J., Chakrabarti, S., 2002. HiRISE: a ground-based high-resolution imaging spectrograph using Echelle grating for measuring daytime airglow and auroral emissions. *Journal of Atmospheric and Solar–Terrestrial Physics* 64, 1581–1587.
- Pallamraju, D., Chakrabarti, S., Doe, R., Pedersen, T., 2004. First ground-based OI 630.0 nm optical measurements of daytime cusp-like and F-region auroral precipitation. *Geophysics Research Letters* 31, L08807.
- Rees, M.H., 1989. Antarctic upper atmosphere investigations by optical methods. *Planetary and Space Science* 37, 95–966.
- Samson, J.C., Lyons, L.R., Newell, P.T., Creuzberg, F., Xu, B., 1992. Proton aurora and substorm intensifications. *Geophysics Research Letters* 19, 2167.
- Sato, N., Fujii, R., Ono, T., Fukunishi, H., Hirasawa, T., Araki, T., Kokubun, S., Makita, K., Saemundsson, Th., 1986. Conjugacy of proton and electron auroras observed near  $L = 6.1$ . *Geophysics Research Letters* 13, 1368–1371.
- Sharber, J.R., Frahm, R.A., Winningham, J.D., Biard, J.C., Lummerzheim, D., Rees, M.H., Chenette, D.L., Gaines, E.E., Nightingale, R.W., Imhof, W.L., 1993. Observations of the UARS particle environment monitor and computation of ionization rates in the middle and upper atmosphere during a geomagnetic storm. *Geophysics Research Letters* 20, 1319–1322.
- Sigernes, F., Fasel, G., Minow, J., Deehr, C.S., Smith, R.W., Lorentzen, D.A., Wetjen, L.T., Henriksen, K., 1996a. Calculations and ground-based observations of pulsed proton events in the dayside aurora. *Journal of Atmospheric and Terrestrial Physics* 58, 1281–1291.
- Sigernes, F., Svenøe, T., Lorentzen, D.A., Sigernes, L.T.W., 1996b. An upgrade of the auroral Ebert–Fastie spectrometer, in optical studies of proton aurora, Ph.D. Thesis, Paper IX, University of Tromsø, Tromsø, Norway.
- Sivjee, G.G., Romick, G.J., Rees, M.H., 1979. Intensity ratio and center wavelengths of OII (7320–7330 Å) line emissions. *Astrophysics Journal* 229, 432.
- Solomon, S.C., 2001. Auroral particle transport using Monte Carlo and hybrid methods. *Journal of Geophysical Research* 106, 107.
- Søraas, F., Lindalen, H.R., Måseide, K., Egeland, A., Sten, T.A., Evans, D.S., 1974. Proton precipitation and the  $H_{\beta}$  emission in a postbreakup auroral glow. *Journal of Geophysical Research* 79, 1851–1859.
- Strickland, D.J., Daniell, R.E., Jasperse, J.R., Basu, B., 1993. Transport theoretic model for the electron-proton-hydrogen atom Aurora, 2, Model results. *Journal of Geophysical Research* 98, 21533.
- Synnes, S.A., Søraas, F., Hansen, J.P., 1998. Monte–Carlo simulations of proton aurora. *Journal of Atmospheric and Solar–Terrestrial Physics* 60, 1695.
- Takahashi, Y., Fukunishi, H., 2001. The dynamics of the proton aurora in auroral breakup events. *Journal of Geophysical Research* 106, 45–63.
- Vallance Jones, A., Creutzberg, F., Gattinger, R.L., Harris, F.R., 1982. Auroral studies with a chain of meridian-scanning photometers. 1. Observations of proton and electron aurora in magnetospheric substorms. *Journal of Geophysical Research* 87, 4489–4503.
- Van Zyl, B., Neumann, H., 1980.  $H_{\alpha}$  and  $H_{\beta}$  emission cross sections for low-energy H and  $H^{+}$  collisions with  $N_2$  and  $O_2$ . *Journal of Geophysical Research* 85, 6006.
- Vegard, L., 1939. Hydrogen showers in the auroral region. *Nature* 144, 1089–1090.
- Vegard, L., 1948. Emission spectra of night sky and aurora. Reports of the Gassiot Committee. The Physical Society of London, p. 82.
- Vonrat-Reberac, A., Fontaine, D., Brelly, P.-L., Galand, M., 2001. Theoretical predictions of cusp and dayside precipitations on the polar ionosphere. *Journal of Geophysical Research* 106, 28,857–28,865.
- Voronkov, I., Donovan, E.F., Jackel, B.J., Samson, J.C., 2000. Large-scale vortex dynamics in the evening and midnight auroral zone: Observations and simulations. *Journal of Geophysical Research* 105, 18,505–18,518.
- Wanliss, J.A., Samson, J.C., Friedrich, E., 2000. On the use of photometer data to map dynamics of the magnetotail current sheet during substorm growth phase. *Journal of Geophysical Research* 105, 27,673–27,684.
- Yousif, F.B., Geddes, J., Gilbody, H.B., 1986. Balmer  $\alpha$  emission in collisions of H,  $H^{+}$ ,  $H_2^{+}$  with  $N_2$ ,  $O_2$ , and  $H_2O$ . *Journal of Physics B* 19, 217.
- Zhang, Y., Paxton, L.J., Meng, C.-I., Morrison, D., Wolven, B., Kil, H., Christensen, A.B., 2004. Double dayside detached auroras: TIMED/GUVI observations. *Geophysics Research Letters* 31, 1.